

Direct Writing of Half-Meter Long CNT Based Fiber for Flexible Electronics

Sihan Huang,[†] Chunsong Zhao,[†] Wei Pan,^{*,†} Yi Cui,[‡] and Hui Wu^{*,†}

[†]State Key Laboratory of New Ceramics and Fine Processing, School of Materials Science and Engineering, Tsinghua University, Beijing 100084, China

[‡]Department of Materials Science and Engineering, Stanford University, Stanford, California 94305, United States

S Supporting Information

ABSTRACT: Rapid construction of flexible circuits has attracted increasing attention according to its important applications in future smart electronic devices. Herein, we introduce a convenient and efficient “writing” approach to fabricate and assemble ultralong functional fibers as fundamental building blocks for flexible electronic devices. We demonstrated that, by a simple hand-writing process, carbon nanotubes (CNTs) can be aligned inside a continuous and uniform polymer fiber with length of more than 50 cm and diameters ranging from 300 nm to several micrometers. The as-prepared continuous fibers exhibit high electrical conductivity as well as superior mechanical flexibility (no obvious conductance increase after 1000 bending cycles to 4 mm diameter). Such functional fibers can be easily configured into designed patterns with high precision according to the easy “writing” process. The easy construction and assembly of functional fiber shown here holds potential for convenient and scalable fabrication of flexible circuits in future smart devices like wearable electronics and three-dimensional (3D) electronic devices.



KEYWORDS: Ultralong fibers, aligned CNTs, controlled assembly, flexible electronics

Flexibility of electronic devices is desired for future smart electronic devices including flexible displays,¹ flexible solar cells,^{2,3} radio frequency identification,⁴ and sensor tapes.⁵ For example, transparent and flexible conducting thin films⁶ enable touch displays to be bent and folded while maintaining their electronic performance. Flexible capacitors^{7,8} and batteries⁹ allow the storage and conversion of energy to be applied in multiple mechanical environments. Wearable systems,^{10,11} such as personal health monitors and medical therapeutics, have greatly improved human health. For these flexible electronic device applications, conducting wires with high conductivity as well as mechanical flexibility play an important role as essential building blocks for constructing the circuits. Especially, breaking the length limit is important because ultralong fibers hold irreplaceable advantages not only in manufacturing efficiency, but also in the fabrication of large-sized flexible electronics. To achieve mechanical flexibility in conventionally rigid electrical systems, micro/nanoscale one-dimensional (1D) structures have been intensively investigated and demonstrated to be important candidates as conducting wires.¹² Deformable interconnects with serpentine designs on prestrained substrates are developed to realize high system-level mechanical stretchability for electronics.¹³ Some up-to-date techniques that academia have managed to develop are solution blow spinning,¹⁴ self-assembly method,¹⁵ and extrusion polymerization.¹⁶ However, precise position control and the convenient assembly process are yet to be realized in scalable production of

flexible electronics. New technology emerged for fiber alignment in recent years; for example, near-field electrospinning (NFES) exploits stable liquid jets region for controlled fabrication and produces fiber patterns with specific spacing and orientation.^{17,18} However, accurate position control of electrospun nanofibers remains as challenge.

We propose that the fiber-drawing technique holds advantages for precise positioning and direct manipulating of functional nanomaterials. Direct drawing of fibers has been successfully used to construct complex structures, patterns, and grids,^{19–24} whereas the procedures are still complicated and the drawing speed is low. Ondarcuhu and Joachim adopted an micropipette to draw a single fiber; however, the maximum length only reached 1 mm, and the drawing rate was limited less than 100 $\mu\text{m/s}$.¹⁹ Suryavanshi et al. made significant progress in controlled fabrication of extremely long nanofibers.²⁰ In their work, they utilized the meniscus to update drawing method and managed to place the fibers in well-aligned patterns. Generally, the fiber is grown along with the nucleation and precipitation of solute material in the liquid meniscus. Therefore, the practical drawing speed is limited by the rate of solution solidification, which is lower than 1 mm/s. This speed is too low to satisfy the need for large scale manufacturing. In

Received: October 29, 2014

Revised: January 22, 2015

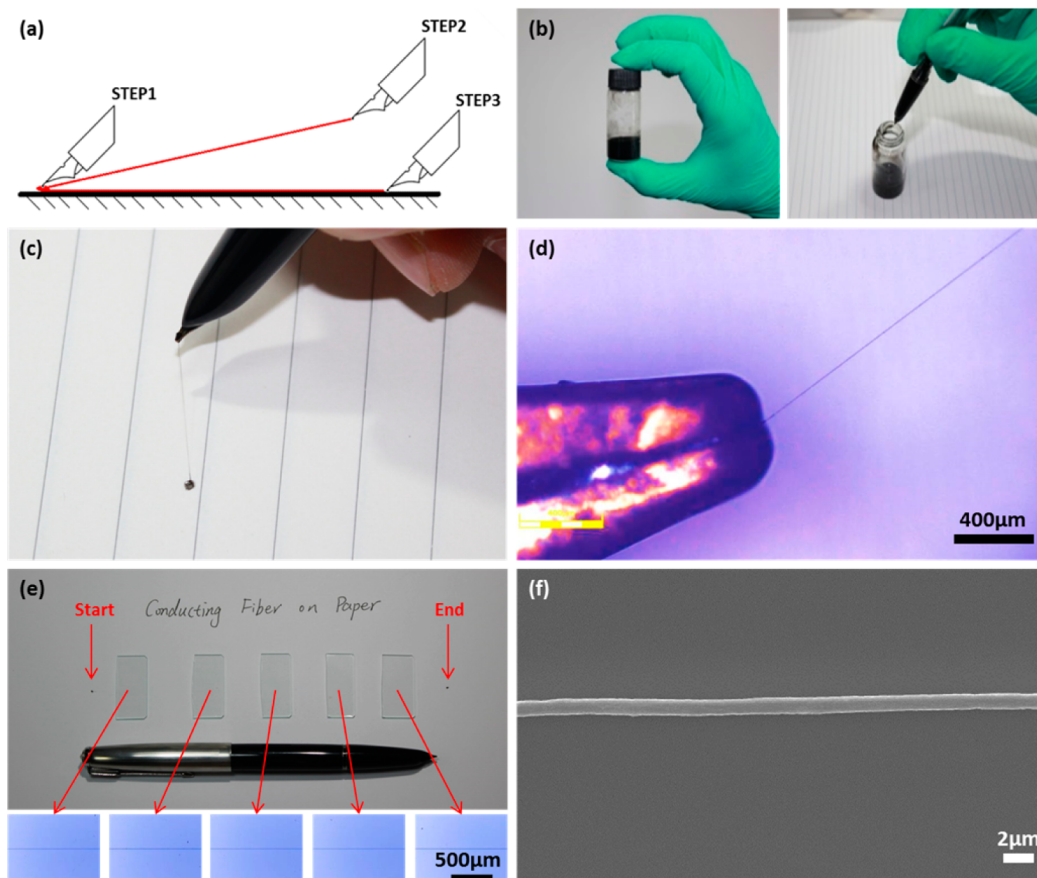


Figure 1. Details and outcomes of the direct writing method. (a) A schematic show of the manufacturing procedure; (b) The ink used for injecting into the pen; (c) Directly drawing a submicron fiber from a pen tip; (d) Optical microscopy of an ultralong fiber being stretched by the pen tip; (e) An ultralong (~ 20 cm) and homogeneous fiber transferred onto glass substrates and the optical microscope images of each segment; (f) SEM image of the fiber in (e) with diameter of around $1 \mu\text{m}$.

order to match the drawing speed, an extra micropipette is needed, which can maintain a stable liquid flow. Besides, precise location control is required throughout the drawing process since the solidified part is not ductile enough.

Herein, we report the functional fibers of CNTs–poly(ethylene oxide) (PEO) composite directly “written” from a pen tip. The fibers can act as highly conductive and flexible conducting wires for flexible microchip circuits. PEO is a crystalline thermoplastic polymer with a molecular weight of up to 8 000 000. Due to its ultrahigh molecular weight, the PEO aqueous solution is highly viscoelastic despite low mass fraction, mechanically strong for pulling continuous fibers from solution. PEO is also compatible with good dispersion of CNTs in aqueous solution. Although PEO is hygroscopic and unstable, it satisfies all of the needs of a prototype perfectly. For polymers of other sorts, the drawing method is more used in large-size macro-fiber dry spinning rather than submicron or nanoscale fiber fabrication, because fibers drawn from the liquid phase are hardly cohesive enough to bear the tensile stress that deform microfibers into nanofibers. As an illustration, fibers directly drawn from a PMMA solution typically have diameters larger than $10 \mu\text{m}$, since a high concentration of the solution is required to achieve a high viscosity.²⁴ To achieve thinner fibers of PEO, surfactants such as sodium dodecyl sulfonate have been added to the solution to lower the surface tension. By employing surfactants, highly diluted (<0.4 wt %) PEO solution can be stretched to form thin fibers with diameter down to

nanosize. In our experiments, we draw fiber from a typical pen tip by using PEO solution as the “ink”, and thin fibers can be stretched from the pen tip, and the suspended fiber can be easily transferred to a substrate after drying (Figure 1a, b and c, Supporting Information, Figure S1). Note that the solvent evaporates rapidly after drawing fibers according to the large specific surface area of thin fiber. Ultimately, the fibers shrink drastically according to the water evaporation, and their diameters decrease to ~ 60 nm (Supporting Information, Figure S2). We note that, in our manufacturing process, PEO solution can be conveniently loaded into the pen similar to ordinary ink (Figure 1b), making our method easy for scalable fiber fabricating.

Our fiber writing process holds several further advantages compared with previous reported drawing methods. First, our fabrication procedure is more efficient, since the drawing speed reaches 10 cm/s and the total time needed to produce one fiber is primarily the time of suspension. It is known that thin fibers are usually fragile and can be easily broken by large tensile stress at high drawing speed. In our process, the presolidification fiber, which have diameters above $1 \mu\text{m}$, remained continuous at a fast drawing up to 10 cm/s. Second, a micropipette is not used in our process since the deformation of fibers is completed while the fibers were still in liquid phase. As a comparison, real-time precise positioning of the micropipette are required for previous fiber drawing methods.

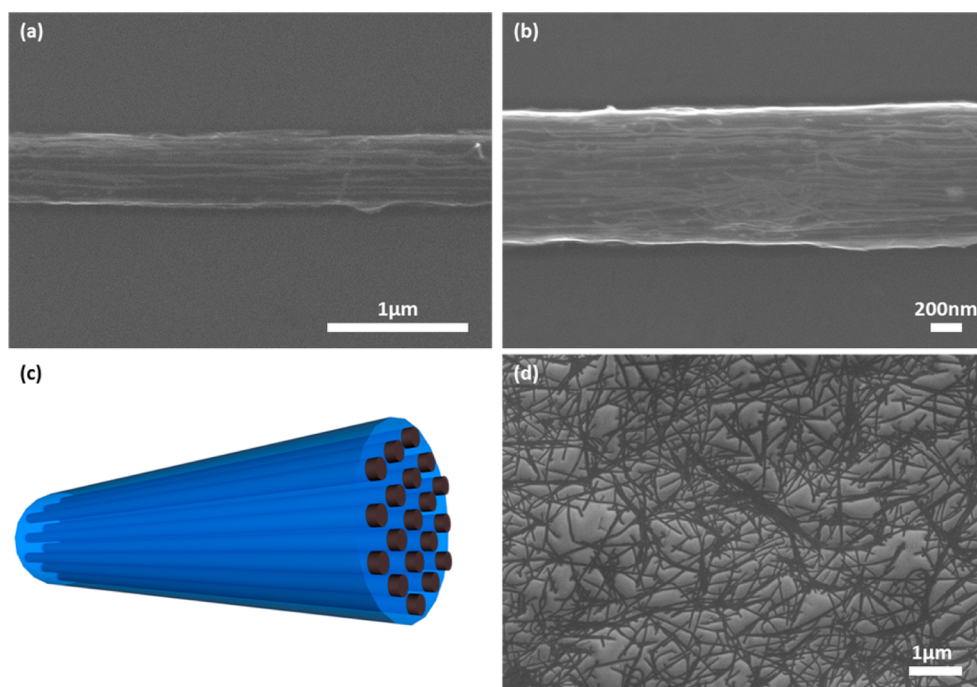


Figure 2. CNT configuration in fibers of different diameters and in the solution-cast film. (a) CNTs configuration in a ~ 300 nm fiber; (b) CNTs configuration in a ~ 1 μm fiber, and entanglements are observed; (c) A schematic 3D figure of idealized distribution of CNTs; (d) SEM of the film showing that the arrangement of CNTs is homogeneous and isotropic.

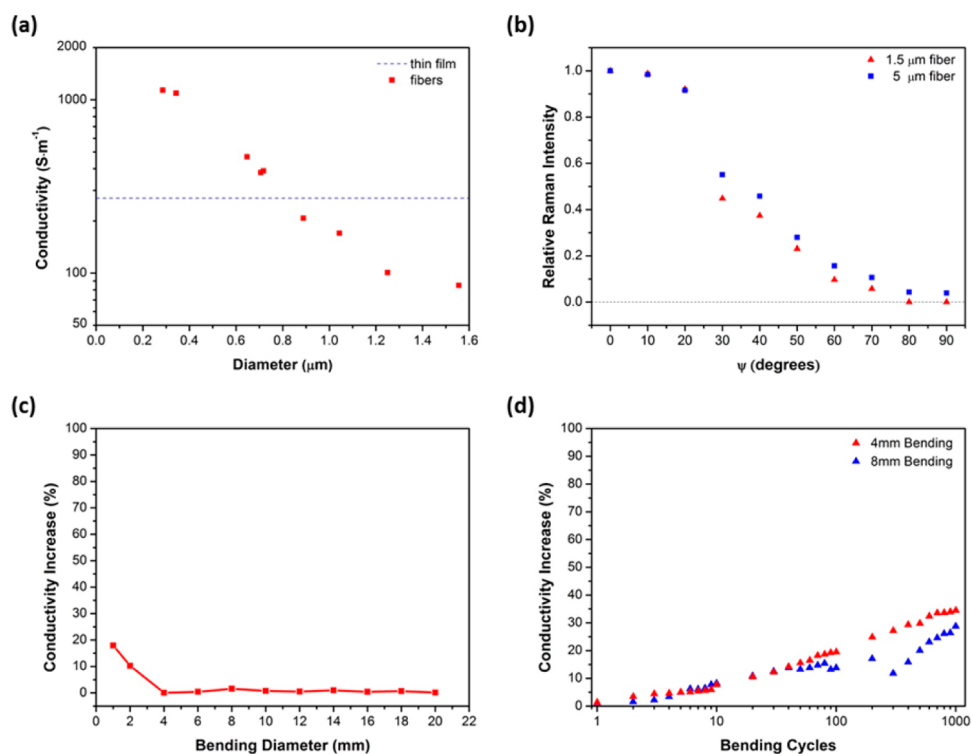


Figure 3. Electrical conductivity and flexibility measurement. (a) Dependence of fiber's conductivity on diameter, blue dotted line indicates the conductivity of a solution-cast film; (b) measured G^+ mode peak intensity (1592 cm^{-1}) as a function of fiber angle Ψ for two fibers which have the same composite but different diameters; (c) electrical performances plotted against bending diameters, measured with a fiber on the PET substrate. (d) Electrical performances plotted against the number of cycles that the fibers are bent, to 4 mm and 8 mm in diameter, respectively.

To achieve electrical conductivity for the hand-written fibers, we dispersed CNTs into PEO solution. Using PEO–CNTs solution (0.3 wt % PEO dissolved in 0.1 wt % single-walled CNTs aqueous solution, 0.3 wt % dispersant) (Figure 1b),

uniform fibers of PEO–CNT can be easily draw from a pen tip with length of over a half meter (Figure 1c and d). Figure 1e shows a uniform single fiber collected on glass slides, crossing 20 cm distance. Figure 1f shows SEM image of a single fiber

with diameter of $\sim 1 \mu\text{m}$. The diameter of a PEO–CNTs fiber can be controlled from $\sim 300 \text{ nm}$ to $\sim 3 \mu\text{m}$ by tuning the concentration of precursor solution (Supporting Information, Figure S3). Using a solution with lower polymer concentration, we can minimize the fiber diameter to be less than 300 nm with length of more than 10 cm (Supporting Information, Figure S2).

We examined the alignment of CNTs in PEO fiber by high-resolution SEM (HRSEM) images as shown in Figure 2. Clearly, carbon nanotubes are highly aligned along the fiber long axis (Figure 2a). Some imperfections of the alignment, such as inhomogeneity and entanglement, are also found in the fibers with higher diameters (Figure 2b). The arrangement of CNTs in these fibers appeals to us, in both its cause and application. The dispersion and alignment of both single-walled and multiwalled CNTs in polymers have been investigated in past years;^{25–31} particularly, the alignment of CNTs (as illustrated in Figure 2c) under stress or within an elongated fiber can be understood by considering the shearing force.^{25–29} For practical applications, CNT based conducting wires need to be optimized to achieve high conductivity, accordingly, the impact of CNT alignment on the electrical conductivity of composite fiber needs further investigation. In our experiments, we found that the resistivity along the axis is related to the fiber diameter. PEO–CNTs fibers of different diameters are prepared and transferred on glass substrates. Two silver electrodes were deposited on the fiber, and the space between two silver electrodes were measured with an optical microscope. The conductivity of the composite fiber is calculated from the fiber resistance and diameter, as shown in Figure 3a. Note that resistances are measured 96 h after fiber deposition (Supporting Information Figure S4). The highest conductivity is $1136.5 \text{ S}\cdot\text{m}^{-1}$, relatively low compared to bulk conductors. That is because CNTs are not typically in direct contact in the composite structure. For comparison, we measured the resistivity of an isotropic PEO–CNTs thin film sample prepared by spin coating. We confirm that CNTs are randomly distributed in the thin film by SEM imaging (Figure 2d), and we determine the thickness of the film by SEM (Supporting Information, Figure S5). The conductivity of the film sample is measured to be $\sigma = 270.4 \text{ S}\cdot\text{m}^{-1}$, as indicated in Figure 3a. Obviously, thinner fibers show better conductivity than thicker ones and even significantly enhanced conductivity compared with isotropic CNT thin film samples.

Our results can be understood by considering the mechanical, morphological, and electrical features of carbon nanotubes. As single CNT is highly anisotropic, due to the cylindrical shape, the overall conductivity of plentiful CNTs is better when they are more perfectly aligned along the axis. The shear stress is larger in thinner fibers, so there are less imperfections of alignment, such as entanglements and inhomogeneity, in thinner fibers (Figure 2a) than in thicker ones (Figure 2b). We quantify the alignment of CNTs by polarized Raman spectroscopy. As previous study has shown,²⁵ the intensity of CNTs' $1592 \text{ cm}^{-1} \text{ G}^+$ mode Raman peak is a function of the angle between the laser polarization direction and the fiber axis. The function is decided by the orientation of CNTs in the fibers. In our experiment, Raman spectra are measured in situ at angles between 0° and 90° on a $1.5\text{-}\mu\text{m}$ fiber and a $5\text{-}\mu\text{m}$ fiber, respectively (Supporting Information, Figure S6). Peak intensities are summarized against fiber angle Ψ in Figure 3b, and the function mentioned above is represented by 10 scatters. Both functions decrease drastically

with increasing angle. However, the one for $1.5\text{-}\mu\text{m}$ -diameter fiber is steeper, while the other one has observable nonzero value at 90° . These facts agree with the information from HRSEM that CNTs are aligned in as-prepared fibers and the orientation is better in thinner fibers. This explains why thinner fibers typically show higher conductivity than thicker fibers and why thin fibers are more conductive than solution-cast film in Figure 3a. The imperfections of CNTs alignment in thick fibers cause lower conductivity than the isotropic film.

The flexible conductivity of a single fiber is expected to be stable, regardless of bending or distortion, so that they are capable of being assembled into flexible devices in multiple situations. Both the flexibility of single fibers and devices' textile-like structure are crucial in flexible electronics manufacturing. To characterize the fibers' flexibility, the steps that follow are taken. In step 1, a suspended fiber is transferred onto a rectangular polyethylene terephthalate (PET) substrate, roughly in the direction of the longer edge. In step 2, two silver paste electrodes covering the fiber beneath them are prepared, and the separation distance is several millimeters. Fibers are fully dried after 96 h. In step 3, the PET substrate is bent to the surface of a cylinder, of which the axis is perpendicular to the fiber. After 20 s, the substrate is allowed to recover freely, and resistance R_f is measured afterward. The steps above are repeated with diameter of the cylinder decreasing in sequence. The percentage increases of conductance from G_{unbent} to G_{d} are plotted against bending diameters, as shown in Figure 3c. Apparently, the single fibers attached to PET substrates can usually bear a curvature down to 4 mm without significant change of conductivity. Even when it is extremely bent to 1 mm, the increase in conductivity is within 20%. Another crucial factor is the performance change when the fiber is bent repeatedly, as is often the case for flexible electronics. Using similar experiments but changing 20 s holding time to 1 s, we derive Figure 3d, in which the two groups of dots indicate bending diameter of 4 mm and 8 mm, respectively. We conclude that, after 1000 cycles, the percentage conductivity increase is 34.4% for 4 mm bending and 28.7% for 8 mm bending, both tolerable. The red marks are typically above blue marks, which indicates greater change of conductivity for larger bending degree. In addition, increased conductivity after bending is quite contrary to common sense as it appears. We herein propose that the tensile stress during bending can cause microdeformation of the polymer as well as improved alignment of CNTs, thus increasing the conductivity. Moreover, the glass-transition temperature T_g of PEO is near room temperature so the polymer shows viscoelasticity, which we believe will cause those microscopic changes to partly remain and accumulate with repeated bending cycles.

To summarize, these PEO–CNTs fibers show excellent flexibility (Supporting Information, Figure S7), which is crucial for applications in flexible electronics. Note that devices' flexibility depends not only on the fibers' flexibility, but also on the adhesion stability between the fiber and the substrate. In our case, the fiber has a circular cross-sectional shape that may not be very suitable for the fiber's adhesion to the flexible substrate due to low contact area, but electronic encapsulation is expected to alleviate the problem.

An obvious advantage of the fibers produced by direct writing is that each single fiber can be controlled and be accurately placed on substrates. In previous works, homogeneously spaced parallel fibers^{20,23} and delicate fiber grids^{20,24} have been successfully prepared by means of micromanipulator-

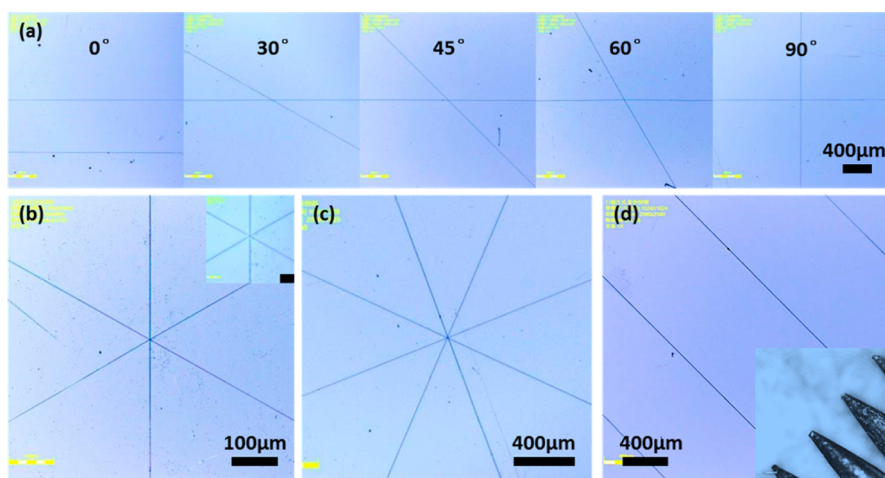


Figure 4. Demonstration of how precisely the fibers are manipulated. (a) Two fibers precisely located to form angles of 0° , 30° , 45° , 60° , and 90° ; (b) three ultralong fibers that cross at one point, also observed to cross well under higher magnification (smaller figure on the top right corner, scale bar $20\ \mu\text{m}$); (c) four ultralong fibers that cross approximately at one point; (d) four parallel ultralong submicron fibers written at one time by four aligned needle tips.

controlled dry spinning. Researchers are capable of directly writing wire bonds, which are free-standing, three-dimensional, and microscaled.²¹ The manipulation of nanofibers is also exhibited by making them into optical nanodevices.²² Our method can achieve convenient and efficient assembly of fiber arrays and can make flexible and conducting circuits across more than 10 cm area. To illustrate the ability of precisely controlling of fibers, we draw conducting fiber lines on a piece of paper with designed patterning. We successfully constructed fiber patterns as shown in Figure 4. Two fibers are precisely located on the central of a glass slide to form angles of 0° , 30° , 45° , 60° , and 90° (Figure 4a). Three fibers are designed to cross at one point, equally dividing 360° into six parts (Figure 4b), and through the smaller graph on the top right corner, we see that they cross well with no significant deviation. Further, we manipulated four continuous fibers crossing at one point (Figure 4c). It is worth mentioning that the crosspoint would have practical electrical functions, if two fibers are prepared in rapid sequence to create merged joints when they are not fully dried, which makes the crosspoint a more reliable electrical connection than mere surface contact. Note that these patterns are realized merely by eye observation, hand operation, and simple coordinate, demonstrating that a precise control of fibers is simple and practicable. We further show that direct writing technology can realize both fast assembly and precise control of ultralong fibers by writing with multiple tips (Figure 4d), which is appealing for rapid and accurate construction of fiber patterns as complex circuits. We believe that our technique can be transplanted to industrial manufacture and more complex fiber patterns can be accomplished by using advanced mechanical devices that can discern and manipulate at submicron level.

In conclusion, by a simple and direct drawing process, we successfully produced ultralong polymer–CNTs composite fibers with length of over 20 cm as precisely controlled conducting wires for flexible electronics. The ultralong submicron fibers can be directly written by ordinary pen, possessing ideal uniformity as well as good alignment of CNTs inside polymer fibers. Our research shows that thinner fibers exhibit higher electrical conductivity according to better alignments of CNTs in fibers. Accurate positioning control and fast assembly have been accomplished conveniently through

this simple writing method. We also demonstrated that such fibers are suitable for flexible electronic device applications with superior mechanical flexibility.

■ ASSOCIATED CONTENT

📄 Supporting Information

Images of a single fiber attached to the needle tip; thinnest fibers fabricated with the most dilute solutions, with and without CNTs; ultralong conductive fibers with tunable diameters, measurement of film thickness; polarized Raman spectra. This material is available free of charge via the Internet at <http://pubs.acs.org>.

■ AUTHOR INFORMATION

Corresponding Authors

*E-mail: huiwu@tsinghua.edu.cn.

*E-mail: panw@tsinghua.edu.cn.

Notes

The authors declare no competing financial interest.

■ ACKNOWLEDGMENTS

This work was supported by National Basic Research of China (Grant No. 2015CB932500 2013CB632702) and NSF of China (Grant No. 51302141).

■ REFERENCES

- (1) Lee, J.; Lee, P.; Lee, H.; Lee, D.; Lee, S. S.; Ko, S. H. *Nanoscale* **2012**, *4* (20), 6408–6414.
- (2) Chen, H.; Zhu, L.; Liu, H.; Li, W. *Nanotechnology* **2012**, *23* (7), 75402.
- (3) Unalan, H. E.; Wei, D.; Suzuki, K.; Dalal, S. *Appl. Phys. Lett.* **2008**, *93* (13), 133116–133116-3.
- (4) Mehdipour, A.; Rosca, I. D.; Sebak, A.; Trueman, C. W.; Hoa, S. *Antennas Wireless Propagation Lett., IEEE* **2010**, *9*, 891–894.
- (5) Wang, X.; Drew, C.; Lee, S.; Senecal, K. J.; Kumar, J.; Samuelson, L. A. *Nano Lett.* **2002**, *2* (11), 1273–1275.
- (6) Wu, H.; Hu, L.; Rowell, M. W.; Kong, D.; Cha, J. J.; McDonough, J. R.; Cui, Y. *Nano Lett.* **2010**, *10* (10), 4242–4248.
- (7) Laforgue, A. *J. Power Sources* **2011**, *196* (1), 559–564.
- (8) Fu, Y.; Cai, X.; Wu, H.; Lv, Z.; Hou, S.; Peng, M.; Zou, D. *Adv. Mater.* **2012**, *24* (42), 5713–5718.

- (9) Altecor, A.; Li, Q.; Lozano, K.; Mao, Y. *Ceram. Int.* **2014**, *40* (3), 5073–5077.
- (10) Shim, B. S.; Chen, W.; Doty, C.; Xu, C.; Kotov, N. A. *Nano Lett.* **2008**, *8* (12), 4151–4157.
- (11) Hu, L.; Pasta, M.; Mantia, F. L.; Cui, L.; Jeong, S.; Deshazer, H. D.; Cui, Y. *Nano Lett.* **2010**, *10* (2), 708–714.
- (12) Choi, K.; Eo, Y.; Kim, K.; Lee, H.; Kim, J. *Fibers Polym.* **2013**, *14* (9), 1556–1561.
- (13) Zhang, Y.; Wang, S.; Li, X.; Fan, J. A.; Xu, S.; Song, Y. M.; Rogers, J. A.; Huang, Y. G. *Adv. Funct. Mater.* **2014**, *24*, 2028–2037.
- (14) Medeiros, E. S.; Glenn, G. M.; Klamczynski, A. P.; Orts, W. J.; Mattoso, L. H. *J. Appl. Polym. Sci.* **2009**, *113* (4), 2322–2330.
- (15) Hartgerink, J. D.; Beniash, E.; Stupp, S. I. *Science* **2001**, *294* (5547), 1684–1688.
- (16) Kageyama, K.; Tamazawa, J.; Aida, T. *Science* **1999**, *285* (5436), 2113–2115.
- (17) Sun, D.; Chang, C.; Li, S.; Lin, L. *Nano Lett.* **2006**, *6* (4), 839–842.
- (18) Pu, J.; Yan, X.; Jiang, Y.; Chang, C.; Lin, L. *Sens. Actuators A: Phys.* **2010**, *164* (1), 131–136.
- (19) Ondarcuhu, T.; Joachim, C. *EPL (Europhys. Lett.)* **1998**, *42* (2), 215.
- (20) Suryavanshi, A. P.; Hu, J.; Yu, M. F. *Adv. Mater.* **2008**, *20* (4), 793–796.
- (21) Hu, J.; Yu, M. *Science* **2010**, *329* (5989), 313–316.
- (22) Xing, X.; Wang, Y.; Li, B. *Opt. Express* **2008**, *16* (14), 10815–10822.
- (23) Nain, A. S.; Sitti, M.; Jacobson, A.; Kowalewski, T.; Amon, C. *Macromol. Rapid Commun.* **2009**, *30* (16), 1406–1412.
- (24) Berry, S. M.; Harfenist, S. A.; Cohn, R. W.; Keynton, R. S. *J. Micromech. Microeng.* **2006**, *16* (9), 1825.
- (25) Haggenueller, R.; Gommans, H. H.; Rinzler, A. G.; Fischer, J. E.; Winey, K. I. *Chem. Phys. Lett.* **2000**, *330* (3), 219–225.
- (26) Jin, L.; Bower, C.; Zhou, O. *Appl. Phys. Lett.* **1998**, *73* (9), 1197–1199.
- (27) Gao, J.; Yu, A.; Itkis, M. E.; Bekyarova, E.; Zhao, B.; Niyogi, S.; Haddon, R. C. *J. Am. Chem. Soc.* **2004**, *126* (51), 16698–16699.
- (28) Wood, J. R.; Zhao, Q.; Wagner, H. D. *Composites Part A: Appl. Sci. Manuf.* **2001**, *32* (3), 391–399.
- (29) Frogley, M. D.; Zhao, Q.; Wagner, H. D. *Phys. Rev. B* **2002**, *65* (11), 113413.
- (30) Chatterjee, T.; Yurekli, K.; Hadjiev, V. G.; Krishnamoorti, R. *Adv. Funct. Mater.* **2005**, *15* (11), 1832–1838.
- (31) Safadi, B.; Andrews, R.; Grulke, E. A. *J. Appl. Polym. Sci.* **2002**, *84* (14), 2660–2669.